condensed matter

MDPI

Article

On the Kinetic Energy Driven Superconductivity in the Two-Dimensional Hubbard Model

Takashi Yanagisawa [1,*], Kunihiko Yamaji [2] and Mitake Miyazaki [1]

[1] National Institute of Advanced Industrial Science and Technology 1-1-1 Umezono, Tsukuba, Ibaraki 305-8568, Japan; miyazaki@hakodate-ct.ac.jp
[2] Hakodate Institute of Technology, 14-1 Tokura, Hakodate, Hokkaido 042-8501, Japan; yamaji@xf7.so-net.ne.jp
* Correspondence: t-yanagisawa@aist.go.jp

Abstract: We investigate the role of kinetic energy for the stability of superconducting state in the two-dimensional Hubbard model on the basis of an optimization variational Monte Carlo method. The wave function is optimized by multiplying by correlation operators of site off-diagonal type. This wave function is written in an exponential-type form given as $\psi_\lambda = \exp(-\lambda K)\psi_G$ for the Gutzwiller wave function ψ_G and a kinetic operator K. The kinetic correlation operator $\exp(-\lambda K)$ plays an important role in the emergence of superconductivity in large-U region of the two-dimensional Hubbard model, where U is the on-site Coulomb repulsive interaction. We show that the superconducting condensation energy mainly originates from the kinetic energy in the strongly correlated region. This may indicate a possibility of high-temperature superconductivity due to the kinetic energy effect in correlated electron systems.

Keywords: strongly correlated electrons; mechanism of superconductivity; high-temperature superconductor; two-dimensional Hubbard model; optimization variational Monte Carlo method; Hubbard model

Citation: Yanagisawa, T.; Yamaji, K.; Miyazaki, M. On the Kinetic Energy Driven Superconductivity in the Two-Dimensional Hubbard Model. *Condens. Matter* **2021**, *6*, 12. https://doi.org/10.3390/condmat6010012

Received: 16 October 2020
Accepted: 22 February 2021
Published: 26 February 2021

1. Introduction

It is important and challenging to clarify the mechanism of high-temperature superconductivity in cuprates. It has been studied intensively for more than three decades [1]. In the study of cuprate high-temperature superconductivity, it is important to understand the ground state phase diagram. For this purpose, we should investigate electronic models with strong correlation.

It is certain that the CuO_2 plane plays an important role in the emergence of high-temperature superconductivity [2–8]. The CuO_2 plane contains oxygen atoms and copper atoms; thus, the CuO_2 plane can be modeled by the d-p model (or the three-band Hubbard model) [9–25]. The single-band Hubbard model [26–28] is important since it can be regarded as a simplified model of the three-band d-p model and may contain important physics concerning high-temperature superconductivity [29–49]. The Hubbard model was first proposed by Hubbard to describe the metal-insulator transition [50] and has been one of the important fundamental models in condensed matter physics up to now. It may contain important physics concerning high-temperature cuprates, such as antiferromagnetic insulator, superconductivity, stripes [51–58], and inhomogeneous states [59–62].

We employ an optimization variational Monte Carlo method to investigate the ground state of the 2D Hubbard model. In a variational Monte Carlo method, we use variational wave functions with strong correlation between electrons [33,34,36–39]. A variational wave function is improved by introducing correlation operators. The wave function used in this paper is obtained by multiplying the Gutzwiller function by $\exp(-\lambda K)$ operators, where K is the kinetic part of the Hamiltonian [47,48,63,64]. We can optimize the wave function further by multiplying by exponential-type operators again [63]. The ground-state energy is lowered greatly with this wave function [47].

The kinetic energy-driven mechanism of superconductivity has been examined in the study of cuprate superconductors for the Hubbard model [42,65–67] and the t-J model [68–70]. This is an interesting subject since there is a possibility that kinetic energy pairing occurs in high-temperature cuprates. In this paper, we discuss the role of kinetic energy based on the improved wave function for the Hubbard model. We evaluate the superconducting condensation energy as a sum of the kinetic and Coulomb energy contributions, and we show that the kinetic energy contribution dominates the condensation energy in the strongly correlated region of large U.

2. Hubbard Hamiltonian

We investigate the two-dimensional Hubbard model. The Hamiltonian of the Hubbard model is

$$H = \sum_{ij\sigma} t_{ij} c^{\dagger}_{i\sigma} c_{j\sigma} + U \sum_{i} n_{i\uparrow} n_{i\downarrow}, \tag{1}$$

where t_{ij} indicates the transfer integral, and U is the strength of the on-site Coulomb interaction. The transfer integral is $t_{ij} = -t$ when i and j are nearest-neighbor pairs $\langle ij \rangle$. We put $t' = 0$ in this paper, where $t_{ij} = -t'$ when i and j are next-nearest neighbor pairs. N and N_e denote the number of lattice sites and the number of electrons, respectively. The energy unit is given by t. We define the non-interacting part as K:

$$K = \sum_{ij\sigma} t_{ij} c^{\dagger}_{i\sigma} c_{j\sigma}. \tag{2}$$

When two electrons with spin up and down are at the same site, the energy becomes higher by U. This simple interaction may cause many interesting phenomena, such as the metal-insulator transition, antiferromagnetic magnetism, and superconductivity.

The metal-insulator transition occurs at half filling when U is as large as the bandwidth. The effective Hamiltonian is given by the Heisenberg model when U is large in the half-filled case, which leads to the t-J model when holes are doped. Magnetic properties of materials may be described by the Hubbard model by introducing suitable magnetic orders. We discuss superconductivity in the strongly correlated region in this paper. The emergence of superconducting state in this region is closely related to the kinetic energy gain that increases as U increases.

3. Optimized Wave Function

In a variational Monte Carlo method, we calculate the expectation values of physical properties by using a Monte Carlo procedure. We start with the Gutzwiller wave function to take account of electron correlation. The Gutzwiller wave function is

$$\psi_G = P_G \psi_0, \tag{3}$$

where P_G is the Gutzwiller operator $P_G = \prod_j (1 - (1 - g) n_{j\uparrow} n_{j\downarrow})$, where g is the variational parameter in the range of $0 \leq g \leq 1$. ψ_0 indicates a one-particle state, such as the Fermi sea, the BCS state, and the antiferromagnetic state.

We improve the wave function by multiplying by the correlation operator given as [47,63,71–75]

$$\psi_\lambda = \exp(-\lambda K) \psi_G, \tag{4}$$

where K is the kinetic part of the Hamiltonian, and λ is a real variational operator [39,63,72].

There are other methods to improve the Gutzwiller wave function by using Jastrow-type operators [41,76,77]. This operator is written as

$$P_{Jdh} = \prod_j \left(1 - (1 - \eta) \prod_\tau \left[d_j (1 - e_{j+\tau}) + e_j (1 - d_{j+\tau}) \right] \right), \tag{5}$$

where d_j is the operator for the doubly-occupied site given as $d_j = n_{j\uparrow}n_{j\downarrow}$, and e_j is that for the empty site given by $e_j = (1-n_{j\uparrow})(1-n_{j\downarrow})$. η is the variational parameter that takes the value in the range of $0 \leq \eta \leq 1$. τ indicates a vector connecting nearest-neighbor sites. The Jastrow-type wave function is written as $\psi_J = P_{Jdh}\psi_G$. An important difference between ψ_λ and ψ_J is that P_{Jdh} is the site-diagonal operator, while ψ_λ is the site-off diagonal operator. The one-particle state ψ_0 is written in the form

$$\psi_0 = \sum_j a_j^0 \varphi_j^0, \tag{6}$$

where $\{\varphi_j^0\}$ is a set of basis functions of the one-particle state in the site representation on a lattice, with j being the label for the electron configuration. ψ_λ and ψ_J are given as

$$\psi_\lambda = \sum_j a_j^0 e^{-\lambda K} P_G \varphi_j^0, \tag{7}$$

$$\psi_J = \sum_j a_j^0 P_{Jdh} P_G \varphi_j^0. \tag{8}$$

Since P_G and P_{Jdh} are diagonal operators, ψ_J is written as

$$\psi_J = \sum_j a_j^J \varphi_j^0, \tag{9}$$

where $a_j^J = a_j^J(g,\eta)$ is determined by parameters g and η. ψ_J is given by a wave function, where the coefficients $\{a_j^0\}$ are modified in the one-particle state. Instead, ψ_λ is not so simple because $e^{-\lambda K}$ generates other basis states from φ_j^0, which means that off-diagonal elements $\langle \varphi_i^0 K \varphi_j^0 \rangle$ are effectively taken into account. We write ψ_λ as

$$\psi_\lambda = \sum_j a_j^\lambda \varphi_j, \tag{10}$$

where the set of basis states $\{\varphi_j\}$ may contain basis states which are not included in $\{\varphi_j^0\}$ since some coefficients a_ℓ^0s may vanish accidentally.

The expectation values are calculated numerically by using the auxiliary field method following a Monte Carlo algorithm [63,78]. We show the ground-state energy per site as a function of U for ψ_G and ψ_λ in Figure 1. The energy is lowered due to the exponential factor $e^{-\lambda K}$. In the region of large U, the energy lowering mainly comes from the kinetic energy gain, as shown later.

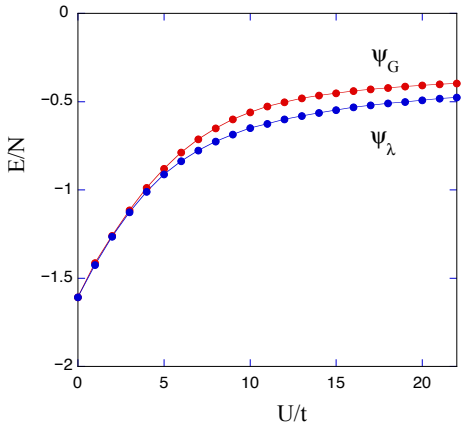

Figure 1. Ground-state energy as a function of U on a 10×10 lattice, where we set $N_e = 88$ and $t' = 0$ with the boundary condition in one direction, and the antiperiodic one in the other direction.

4. Correlated Superconducting State

The correlated superconducting state is obtained by multiplying the BCS wave function by a correlation operator. The BCS wave function is

$$\psi_{BCS} = \prod_k (u_k + v_k c^\dagger_{k\uparrow} c^\dagger_{-k\downarrow})|0\rangle, \tag{11}$$

with coefficients u_k and v_k that appear in the ratio $u_k/v_k = \Delta_k/(\xi_k + \sqrt{\xi_k^2 + \Delta_k^2})$, where Δ_k is the gap function with $\mathbf{k}$ dependence, and $\xi_k = \epsilon_k - \mu$ is the dispersion relation of conduction electrons. We adopt the d-wave symmetry for Δ_k, and we do not consider other symmetries in this paper since an SC state with other symmetry unlikely becomes stable in the simple single-band Hubbard model. The Gutzwiller BCS state is given by

$$\psi_{G-BCS} = P_{N_e} P_G \psi_{BCS}, \tag{12}$$

where P_{N_e} indicates the operator to extract the state with N_e electrons. Here, the total electron number is fixed, and the chemical potential in ξ_k is regarded as a variational parameter.

The improved superconducting wave function is written as

$$\psi_\lambda = e^{-\lambda K} P_G \psi_{BCS}. \tag{13}$$

In the formulation of ψ_λ, we cannot fix the total electron number, and we should use a different Monte Carlo sampling procedure. We perform the electron-hole transformation for down-spin electrons:

$$d_k = c^\dagger_{-k\downarrow}, \quad d^\dagger_k = c_{-k\downarrow}, \tag{14}$$

and not for up-spin electrons: $c_k = c_{k\uparrow}$. In the real space, we have $c_i = c_{i\uparrow}$ and $d_i = c^\dagger_{i\downarrow}$.

The electron pair operator $c^\dagger_{k\uparrow} c^\dagger_{-k\downarrow}$ is transformed to the hybridization operator $c^\dagger_k d_k$. Then, we can use the auxiliary field method after this transformation in a Monte Carlo simulation. This is performed by expressing the Gutzwiller operator in the form [72].

$$\begin{aligned} P_G &= \prod_i (1 - (1-g) c^\dagger_i c_i (1 - d^\dagger_i d_i)) \\ &= \prod_i \exp(-\alpha c^\dagger_i c_i + \alpha c^\dagger_i c_i d^\dagger_i d_i) \\ &= \left(\frac{1}{2}\right)^N \sum_{s_i = \pm 1} \exp\Big[\sum_i (2a s_i - \alpha/2)(c^\dagger_i c_i - d^\dagger_i d_i)\Big], \end{aligned} \tag{15}$$

where $g = e^{-\alpha}$, $\cosh(2a) = e^{-\alpha/2}$, and s_i is the auxiliary field that takes the value of ± 1. By using this form, the expectation value is calculated as a sum of terms with respect to auxiliary fields, for which we apply the Monte Carlo procedure [63,72].

5. Kinetic Energy in the Superconducting State

In this section, we discuss the role of kinetic energy in the superconducting state in the two-dimensional Hubbard model. We consider the large-U region, where the kinetic energy of electrons would play an important role. Here, large-U means that U is much larger than the band width. The ground-state energy is determined by the balance of the kinetic energy and the Coulomb energy. We show the energy expectation values as a function of λ in Figure 2, where E_g/N is the ground-state energy per site, E_{kin}/N is the expectation value of the non-interacting part of the Hamiltonian $E_{kin} = \langle \psi_\lambda K \psi_\lambda \rangle / \langle \psi_\lambda \psi_\lambda \rangle$, and E_U denotes the Coulomb energy given by $E_U = U \langle \psi_\lambda \sum_i n_{i\uparrow} n_{i\downarrow} \psi_\lambda \rangle / \langle \psi_\lambda \psi_\lambda \rangle$. E_g has a minimum value for a finite value of λ.

The kinetic energy part gives a large contribution to E_g when U is large. This is shown in Figure 3. When $U > 10t$, E_U for ψ_λ almost agrees with that for ψ_G. The difference of

E_{kin} for ψ_λ and ψ_G increases for $U > 10t$. The region that may be called the 'kinetic energy phase' exists when $10 < U/t$.

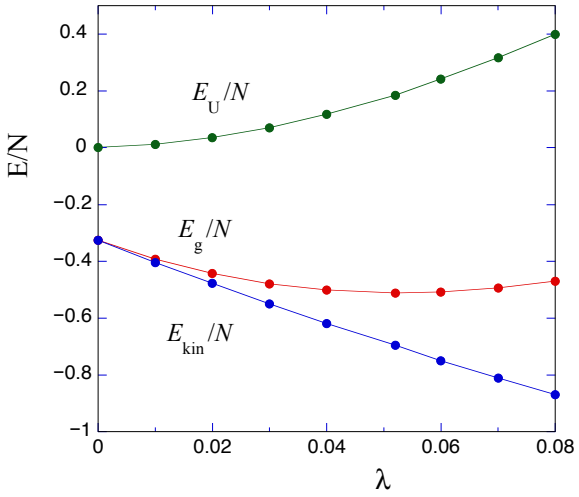

Figure 2. Ground-state energy E_g/N, kinetic energy E_{kin}/N, and the expectation value of the Coulomb interaction E_U/N as a function of λ on a 10×10 lattice with the periodic boundary condition in one direction, and the antiperiodic one in the other direction. We set $N_e = 88$, $U = 18t$ and $t' = 0$.

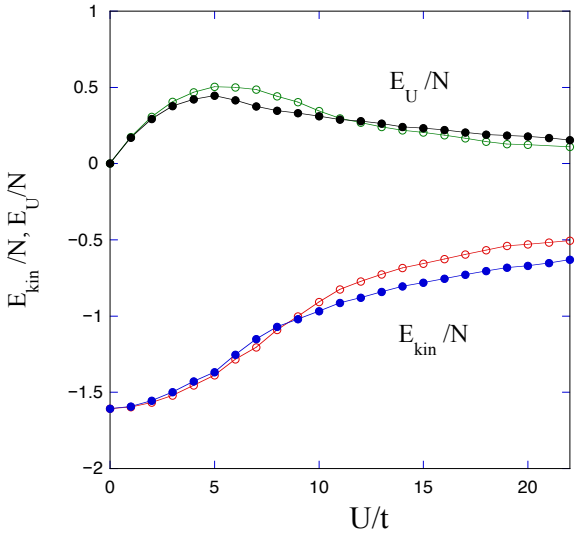

Figure 3. Kinetic energy E_{kin}/N and the Coulomb energy E_U/N as a function of U on a 10×10 lattice. The boundary conditions are the same as in Figure 2. The electron number is $N_e = 88$, and we put $t' = 0$. Open circles indicate the results for the Gutzwiller function, and solid circles are those for the improved ψ_λ.

Let us consider the the difference of the kinetic energy defined as

$$\Delta E_{kin} = E_{kin}(\psi_G) - E_{kin}(\psi_\lambda), \tag{16}$$

where $E_{kin}(\psi_G)$ and $E_{kin}(\psi_\lambda)$ denote the kinetic energy for ψ_G and ψ_λ, respectively. Since $\psi_G = \psi_{\lambda=0}$ with vanishing λ, we can write $\Delta E_{kin} = E_{kin}(\lambda = 0) - E_{kin}(\lambda)$ for the optimized value λ. We show $\Delta E_{kin}/N$ as a function of U in Figure 4, where the hole doping rate x is $x = 0.12$. ΔE_{kin} begins to increase when U is of the order of the band width $U \sim 8t$. ΔE_{kin} has a broad peak when $15t < U < 20t$. We define the SC condensation energy ΔE_{sc} and the kinetic energy condensation energy ΔE_{kin-sc} as

$$\Delta E_{sc} = E_g(\Delta = 0) - E_g(\Delta = \Delta_{\rm opt}), \quad (17)$$

$$\Delta E_{kin-sc} = E_{kin}(\Delta = 0) - E_{kin}(\Delta = \Delta_{\rm opt}), \quad (18)$$

where $\Delta = \Delta_{sc}$ is the superconducting order parameter, and $\Delta_{\rm opt}$ is its optimized value. We assumed the d-wave symmetry for Δ_k: $\Delta_k = \Delta(\cos k_x - \cos k_y)$. $\Delta E_{kin-sc}/N$ is also shown in Figure 4. The figure indicates that ΔE_{kin-sc} increases for large U, showing a similar behavior to ΔE_{kin}. ΔE_{kin-sc} can change the sign when U is small, which is consistent with the analysis for $Bi_2Sr_2CaCu_2O_{8+\delta}$ [79].

In Figure 5, we show $\Delta E_{kin}/N$ and $\Delta E_{kin-sc}/N$ for $x = 0.20$. ΔE_{kin} for $x = 0.20$ is smaller than that for $x = 0.12$. The kinetic energy condensation energy ΔE_{kin-sc} is also reduced for $x = 0.20$ compared to that for $x = 0.12$. This result inevitably leads to the decrease of the SC condensation energy [48]. Hence, the kinetic energy effect becomes weak when the hole doping rate is large.

The Coulomb energy gain in the presence of the SC order parameter ΔE_{U-sc} is also evaluated, where

$$\Delta E_{U-sc} = E_U(\Delta = 0) - E_U(\Delta = \Delta_{\rm opt}). \quad (19)$$

ΔE_{U-sc} is the Coulomb energy contribution to the SC condensation energy; namely, we have

$$\Delta E_{sc} = \Delta E_{kin-sc} + \Delta E_{U-sc}. \quad (20)$$

Our result shows that

$$\Delta E_{kin-sc} > 0, \quad \Delta E_{U-sc} < 0, \quad (21)$$

for the improved state $\psi_{\lambda-BCS}$. We show the SC condensation energy $\Delta E_{sc}(\Delta_{sc})$ and the Coulomb energy part $\Delta E_{U-sc}(\Delta_{sc})$ as a function of Δ_{sc} in Figure 6 where $\Delta E_{sc}(\Delta) = E_g(\Delta = 0) - E_g(\Delta)$ and $\Delta E_{U-sc}(\Delta) = E_U(\Delta = 0) - E_U(\Delta)$. The positive $\Delta E_{kin-sc} > 0$ indicates that the SC state $\psi_{\lambda-BCS}$ becomes stable due to the kinetic energy effect.

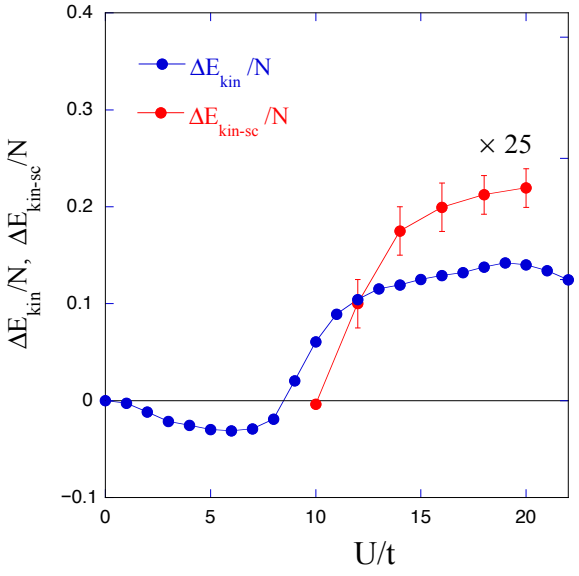

Figure 4. Kinetic-energy difference $\Delta E_{kin}/N$ and the kinetic energy difference in the SC state $\Delta E_{kin-sc}/N$ (×25) as a function of U on a 10×10 lattice. Since $\Delta E_{kin-sc}/N$ is small compared to $\Delta E_{kin}/N$, we multiplied $\Delta E_{kin-sc}/N$ by 25. The boundary conditions are the same as in Figure 1. The electron number is $N_e = 88$ ($n = 0.88$) and we put $t' = 0$.

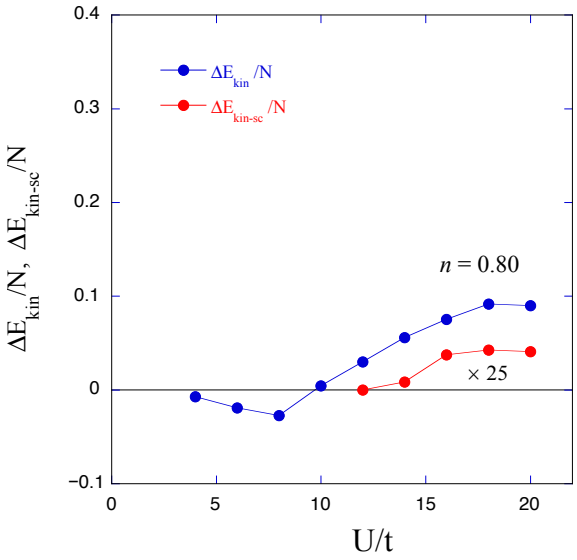

Figure 5. Kinetic-energy difference $\Delta E_{kin}/N$ and the kinetic energy difference in the SC state $\Delta E_{kin-sc}/N$ ($\times 25$) as a function of U on a 10×10 lattice for $N_e = 80$ ($n = 0.80$) and $t' = 0$. The boundary conditions are the same as in Figure 1.

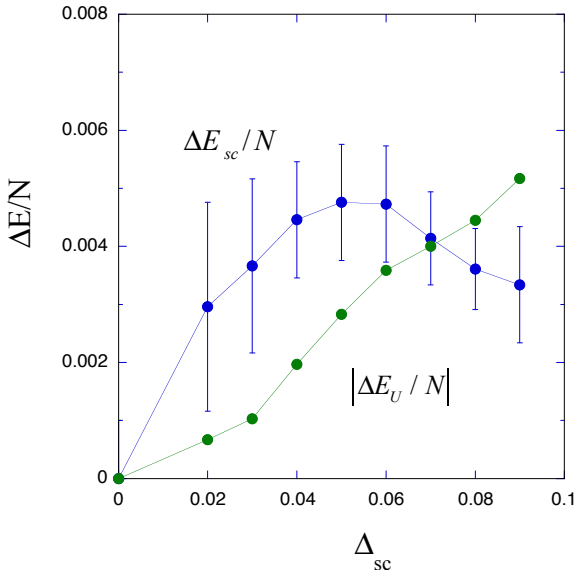

Figure 6. SC condensation energy $\Delta E_{sc}(\Delta_{sc})/N$ and its Coulomb energy part $|\Delta E_{U-sc}(\Delta_{sc})/N|$ as a function of Δ_{sc} on a 10×10 lattice for $N_e = 88$ ($n = 0.88$) and $U = 18$. We set $t' = 0$. ΔE_{U-sc} is negative for this set of parameters. The boundary conditions are the same as in Figure 1.

6. Summary

We investigated the ground state of the two-dimensional Hubbard model by using the optimization variational Monte Carlo method with focus on the strongly correlated large-U region. The ground-state energy is greatly lowered due to the $\exp(-\lambda K)$ correlation operator. The optimization variational Monte Carlo method is effective even in strongly correlated regions where U is much larger than the bandwidth.

In the large-U region, the kinetic energy term becomes dominant in the ground state, and the kinetic energy effect dominates the antiferromagnetic correlation. The kinetic energy difference $\Delta E_{kin} = E_{kin}(\psi_G) - E_{kin}(\psi_\lambda)$ increases when $U > 10t$ and has a broad peak. The kinetic condensation energy ΔE_{kin-sc} behaves like the kinetic energy difference ΔE_{kin} for $U > 10t$. There is a correlation between ΔE_{kin-sc} and ΔE_{kin}. The condensation energy ΔE_{sc} mainly comes from the kinetic energy part ΔE_{kin-sc} and there is a competition between the kinetic energy and the Coulomb energy. Hence there are two competitions

in the Hubbard model; one is that between superconductivity and antiferromagnetism and the other is that between kinetic energy effect and Coulomb repulsive interaction. As a result of competitions, superconducting transition occurs. The result shows that superconductivity in the strongly correlated region is induced by kinetic energy effect. We expect that high-temperature superconductivity would be realized in the strongly correlated region of the two-dimensional Hubbard model.

Author Contributions: Conceptualization, T.Y. and M.M.; Methodology, T.Y. and K.Y.; Validation, T.Y., M.M. and K.Y.; Writing-Original Draft Preparation, T.Y. All authors have read and agreed to the published version of the manuscript.

Funding: This work was supported by a Grant-in-Aid for Scientific Research from the Ministry of Education, Culture, Sports, Science and Technology of Japan (Grant No. 17K05559).

Acknowledgments: A part of computations was supported by the Supercomputer Center of the Institute for Solid State Physics, the University of Tokyo.

Conflicts of Interest: The authors declare no conflict of interest.

Abbreviations

The following abbreviations are used in this manuscript:

VMC	variational Monte Carlo method
AF	antiferromagnetic
SC	superconductivity or superconducting
2D	two-dimensional
AFI	antiferromagnetic insulator
PI	paramagnetic insulator

References

1. Bednorz, J.B.; Müller, K.A. Possible high T_c superconductivity in the Ba-La-Cu-O system. *Z. Phys.* **1986**, *B64*, 189. [CrossRef]
2. McElroy, K.; Simmonds, R.W.; Hoffman, J.E.; Lee, D.H.; Orenstein, J.; Eisaki, H.; Uchida, S.; Davis, J.C. Relating atomic-scale electronic phenomena to wave-like quasiparticle states in superconducting $Bi_2Sr_2CaCu_2O_{8+\delta}$. *Nature* **2003**, *422*, 592. [CrossRef] [PubMed]
3. Hussey, N.E.; Abdel-Jawad, M.; Carrington, A.; Mackenzie, A.P.; Balicas, L. A coherent three-dimensional Fermi surface in a high-transition-temperature superconductor. *Nature* **2003**, *425*, 814. [CrossRef]
4. Weber, C.; Haule, K.; Kotliar, G. Critical weights and waterfalls in doped charge-transfer insulators. *Phys. Rev.* **2008**, *B78*, 134519. [CrossRef]
5. Hybertsen, M.S.; Schlüter, M.; Christensen, N.E. Calculation of Coulomb-interaction parameter for La_2CuO_4 using a constrained-density-functional approach. *Phys. Rev.* **1989**, *B39*, 9028. [CrossRef] [PubMed]
6. Eskes, H.; Sawatzky, G.A.; Feiner, L.F. Effective transfer for singlets formed by hole doping in the high-T_c superconductors. *Physica* **1989**, *C160*, 424. [CrossRef]
7. McMahan, A.K.; Annett, J.F.; Martin, R.M. Cuprate parameters from numerical Wannier functions. *Phys. Rev.* **1990**, *B42*, 6268. [CrossRef] [PubMed]
8. Eskes, H.; Sawatzky, G. Single-, triple-, or multiple-band Hubbard models. *Phys. Rev.* **1991**, *B43*, 119. [CrossRef] [PubMed]
9. Emery, V.J. Theory of high-T_c superconductivity in oxides. *Phys. Rev. Lett.* **1987**, *58*, 2794. [CrossRef]
10. Hirsch, J.E.; Loh, E.Y.; Scalapinom, D.J.; Tang, S. Pairing interaction in CuO clusters. *Phys. Rev.* **1989**, *B39*, 243. [CrossRef]
11. Scalettar, R.T.; Scalapino, D.J.; Sugar, R.L.; White, S.R. Antiferromagnetic, charge-transfer, and pairing correlations in the three-band Hubbard model. *Phys. Rev.* **1991**, *B44*, 770. [CrossRef]
12. Oguri, A.; Asahatam, T.; Maekawa, S. Gutzwiller wave function in the three-band Hubarf model: A variational Monte Carlo study. *Phys. Rev.* **1994**, *B49*, 6880. [CrossRef] [PubMed]
13. Koikegami, S.; Yamada, K. Antiferromagnetic and superconducting correlations on the d-p model. *J. Phys. Soc. Jpn.* **2000**, *69*, 768. [CrossRef]
14. Yanagisawa, T.; Koike, S.; Yamaji, K. Ground state of the three-band Hubbard model. *Phys. Rev.* **2001**, *B64*, 184509. [CrossRef]
15. Koikegami, S.; Yanagisawa, T. Superconducting gap of the two-dimensional d-p model with small U_d. *J. Phys. Soc. Jpn.* **2001**, *70*, 3499. [CrossRef]
16. Yanagisawa, T.; Koike, S.; Yamaji, K. Lattice distortions, incommensurability, and stripes in the electronic model for high-T_c cuprates. *Phys. Rev.* **2003**, *B67*, 132408. [CrossRef]
17. Koikegami, S.; Yanagisawa, T. Superconductivity in Sr_2RuO_4 mediated by Coulomb scattering. *Phys. Rev.* **2003**, *B67*, 134517. [CrossRef]

18. Koikegami, S.; Yanagisawa, T. Superconductivity in multilayer perovskite. *J. Phys. Soc. Jpn.* **2006**, *75*, 034715. [CrossRef]
19. Yanagisawa, T.; Miyazaki, M.; Yamaji, K. Incommensurate antiferromagnetism coexisting with superconductivity in two-dimensional d-p model. *J. Phys. Soc.* **2009**, *78*, 031706. [CrossRef]
20. Weber, C.; Lauchi, A.; Mila, F.; Giamarchi, T. Orbital currents in extended Hubbard model of High-T_c cuprate superconductors. *Phys. Rev. Lett.* **2009**, *102*, 017005. [CrossRef]
21. Lau, B.; Berciu, M.; Sawatzky, G.A. High spin polaron in lightly doped CuO_2 planes. *Phys. Rev. Lett.* **2011**, *106*, 036401. [CrossRef] [PubMed]
22. Weber, C.; Giamarchi, T.; Varma, C.M. Phase diagram of a three-orbital model for high-T_c cuprate superconductors. *Phys. Rev. Lett.* **2014**, *112*, 117001. [CrossRef]
23. Avella, A.; Mancini, F.; Paolo, F.; Plekhanov, E. Emery vs Hubbard model for cuprate superconductors: A composite operator method study. *Eur. Phys. J.* **2013**, *B86*, 265. [CrossRef]
24. Ebrahimnejad, H.; Sawatzky, G.A.; Berciu, M. Differences between the insulating limit quasiparticles of one-band and three-band cuprate models. *J. Phys. Cond. Matter* **2016**, *28*, 105603. [CrossRef]
25. Tamura, S.; Yokoyama, H. Variational study of magnetic ordered state in d-p model. *Phys. Procedia* **2016**, *81*, 5. [CrossRef]
26. Hubbard, J. Electron correlations in narrow energy bands. *Proc. R. Soc. Lond.* **1963**, *276*, 238.
27. Hubbard, J. Electron correlations in narrow energy bands III. *Proc. R. Soc. Lond.* **1964**, *281*, 401.
28. Gutzwiller, M.C. Effect of correlation on the ferromagnetism of transition metals. *Phys. Rev. Lett.* **1963**, *10*, 159. [CrossRef]
29. Zhang, S.; Carlson, J.; Gubernatis, J.E. Constrained path Monte Carlo method for fermion ground states. *Phys. Rev.* **1997**, *B55*, 7464. [CrossRef]
30. Zhang, S.; Carlson, J.; Gubernatis, J.E. Pairing correlation in the two-dimensional Hubbard model. *Phys. Rev. Lett.* **1997**, *78*, 4486. [CrossRef]
31. Yanagisawa, T.; Shimoi, Y. Exact results in strongly correlated electrons. *Int. J. Mod. Phys.* **1996**, *B10*, 3383. [CrossRef]
32. Yanagisawa, T.; Shimoi, Y.; Yamaji, K. Superconducting phase of a two-chain Hubbard model. *Phys. Rev.* **1995**, *B52*, R3860. [CrossRef] [PubMed]
33. Nakanishi, T.; Yamaji, K.; Yanagisawa, T. Variational Monte Carlo indications of d-wave superconductivity in the two-dimensional Hubbard model. *J. Phys. Soc. Jpn.* **1997**, *66*, 294. [CrossRef]
34. Yamaji, K.; Yanagisawa, T.; Nakanishi, T.; Koike, S. Variational Monte Carlo study on the superconductivity in the two-dimensional Hubbard model. *Physica* **1998**, *C304*, 225. [CrossRef]
35. Koike, S.; Yamaji, K.; Yanagisawa, T. Effect of the medium-range transfer energies to the superconductivity in the two-chain Hubbard model. *J. Phys. Soc. Jpn.* **1999**, *68*, 1657. [CrossRef]
36. Yamaji, K.; Yanagisawa,T.; Koike, S. Bulk limit of superconducting condensation energy in 2D Hubbard model. *Physica* **2000**, *B284*, 415–416. [CrossRef]
37. Yamaji, K.; Yanagisawa, T.; Miyazaki, M.; Kadono, R. Superconducting condensation energy of the two-dimensional Hubbard model in the large-negative-t' region. *J. Phys. Soc. Jpn.* **2011**, *80*, 083702. [CrossRef]
38. Hardy, T.M.; Hague, P.; Samson, J.H.; Alexandrov, A.S. Superconductivity in a Hubbard-Fröhlich model in cuprates. *Phys. Rev.* **2009**, *B79*, 212501. [CrossRef]
39. Yanagisawa, T.; Miyazaki, M.; Yamaji, K. Correlated-electron systems and high-temperature superconductivity. *J. Mod. Phys.* **2013**, *4*, 33. [CrossRef]
40. Bulut, N. $d_{x^2-y^2}$ superconductivity and the Hubbard model. *Adv. Phys.* **2002**, *51*, 1587. [CrossRef]
41. Yokoyama, H.; Tanaka, Y.; Ogata, M.; Tsuchiura, H. Crossover of superconducting properties and kinetic-energy gain in two-dimensional Hubbard model. *J. Phys. Soc. Jpn.* **2004**, *73*, 1119. [CrossRef]
42. Yokoyama, H.; Ogata, M.; Tanaka, Y. Mott transitions and d-wave superconductivity in half-filled Hubbard model on square lattice with geometric frustration *J. Phys. Soc. Jpn.* **2006**, *75*, 114706. [CrossRef]
43. Aimi, T.; Imada, M. Does simple two-dimensional Hubbard model account for high-T_c superconductivity in copper oxides? *J. Phys. Soc. Jpn.* **2007**, *76*, 113708. [CrossRef]
44. Miyazaki, M.; Yanagisawa, T.; Yamaji, K. Diagonal stripe states in the light-doping region in the two-dimensional Hubbard model. *J. Phys. Soc. Jpn.* **2004**, *73*, 1643. [CrossRef]
45. Yanagisawa, T. Phase diagram of the t-U^2 Hamiltonian of the weak coupling Hubbard model. *New J. Phys.* **2008**, *10*, 023014. [CrossRef]
46. Yanagisawa, T. Enhanced pair correlation functions in the two-dimensional Hubbard model. *New J. Phys.* **2013**, *15*, 033012. [CrossRef]
47. Yanagisawa, T. Crossover from wealy to strongly correlated regions in the two-dimensional Hubbard model-Off-diagonal Monte Carlo studies of Hubbard model II. *J. Phys. Soc. Jpn.* **2016**, *85*, 114707. [CrossRef]
48. Yanagisawa, T. Antiferromagnetic, Superconductivity and phase diagram in the two-dimensional Hubbard model-Off-diagonal wave function Monte Carlo studies of Hubbard model. *J. Phys. Soc. Jpn.* **2019**, *88*, 054702. [CrossRef]
49. Yanagisawa, T. Mechanism of high-temperature superconductivity in correlated-electron systems. *Condens. Matter* **2019**, *4*, 57. [CrossRef]
50. Mott, N.F. *Metal-Insulator Transitions*; Taylor and Francis Ltd.: London, UK, 1974.

51. Tranquada, J.M.; Axe, J.D.; Ichikawa, N.; Nakamura, Y.; Uchida, S.; Nachumi, B. Neutron-scattering study of stripe-phase order of holes and spins in $La_{1.48}Nd_{0.4}Sr_{0.12}CuO_4$. *Phys. Rev.* **1996**, *B54*, 7489. [CrossRef] [PubMed]
52. Suzuki, T.; Goto, T.; Chiba, K.; Shinoda, T.; Fukase, T.; Kimura, H.; Yamada, K.; Ohashi, M.; Yamaguchi, Y. Observation of modulated magnetic long-range order in $La_{1.88}Sr_{0.12}CuO_4$. *Phys. Rev.* **1998**, *B57*, R3229. [CrossRef]
53. Yamada, K.; Lee, C.H.; Kurahashi, K.; Wada, J.; Wakimoto, S.; Ueki, S.; Kimura, H.; Endoh, Y.; Hosoya, S.; Shirane, G.; et al. Doping dependence of the spatially modulated dynamical spin correlations and the superconducting-transition temperature in $La_{2-x}Sr_xCuO_4$. *Phys. Rev.* **1998**, *B57*, 6165. [CrossRef]
54. Arai, M.; Nishijima, T.; Endoh, Y.; Egami, T.; Tajima, S.; Tomimoto, K.; Shiohara, Y.; Takahashi, M.; Garrett, A.; Bennington, S.M. Incommensurate spin dynamics of underdoped superconductor $YBa_2Cu_3Y_{6.7}$. *Phys. Rev. Lett.* **1999**, *83*, 608. [CrossRef]
55. Mook, H.A.; Dai, P.; Dogan, F.; Hunt, R.D. One-dimensional nature of the magnetic fluctuations in $YBa_2Cu_3O_{6.6}$. *Nature* **2000**, *404*, 729. [CrossRef]
56. Wakimoto, S.; Birgeneau, R.J.; Kastner, M.A.; Lee, Y.S.; Erwin, R.; Gehring, P.M.; Lee, S.H.; Fujita, M.; Yamada, K.; Endoh, Y.; et al. Direct observation of a one-dimensional static spin modulation in insulating $La_{1.95}Sr_{0.05}CuO_4$. *Phys. Rev.* **2000**, *B61*, 3699. [CrossRef]
57. Bianconi, A.; Saini, N.L.; Lanzara, A.; Missori, M.; Rossetti, T.; Oyanagi, H.; Yamaguchi, H.; Oka, K.; Ito, T. Determination of the local lattice distortions in the CuO_2 plane of $La_{1.85}Sr_{0.15}CuO_4$. *Phys. Rev. Lett.* **1996**, *76*, 3412. [CrossRef] [PubMed]
58. Bianconi, A. Quantum materials: Shape resonances in superstripes. *Nat. Phys.* **2013**, *9*, 536. [CrossRef]
59. Hoffman, J.E.; McElroy, K.; Lee, D.-H.; Lang, K.M.; Eisaki, H.; Uchida, S.; Davis, J.C. Imaging quasiparticle interference in $Bi_2Sr_2CaCu_2O_{8+\delta}$. *Science* **2002**, *295*, 466. [CrossRef]
60. Wise, W.D.; Boyer, M.C.; Chatterjee, K.; Kondo, T.; Takeuchi, T.; Ikuta, H.; Wang, Y.; Hudson, E.W. Charge-density-wave origin of cuprate checkerboard visualized by scanning tunnelling microscopy. *Nat. Phys.* **2008**, *4*, 696. [CrossRef]
61. Hanaguri, T.; Lupien, C.; Kohsaka, Y.; Lee, D.H.; Azuma, M.; Takano, M.; Takagi, H.; Davis, J.C. A checkerboard electronic crystal state in lightly hole-doped $Ca_{2-x}Na_xCuO_2Cl_2$. *Nature* **2004**, *430*, 1001. [CrossRef]
62. Miyazaki, M.; Yanagisawa, T.; Yamaji, K. Checkerboard states in the two-dimensional Hubbard model with the Bi2212-type band. *J. Phys. Soc. Jpn.* **2009**, *78*, 043706. [CrossRef]
63. Yanagisawa, T.; Koike, S.; Yamaji, K. Off-diagonal wave function Monte Carlo Studies of Hubbard model I. *J. Phys. Soc. Jpn.* **1998**, *67*, 3867. [CrossRef]
64. Yanagisawa, T.; Miyazaki, M. Mott transition in cuprate high-temperature superconductors. *EPL* **2014**, *107*, 27004. [CrossRef]
65. Maier, T.A.; Jarrell, M.; Macridin, A.; Slezak, C. Kinetic energy driven pairing in cuprate superconductors. *Phys. Rev. Lett.* **2004**, *92*, 027005. [CrossRef]
66. Gull, E.; Millis, A.J. Energetics of superconductivity in the two-dimensional Hubbard model. *Phys. Rev. B* **2012**, *86*, 241106. [CrossRef]
67. Tocchio, L.F.; Becca, F.; Sorella, S. Hidden Mott transition and large-U superconductivity in the two-dimensional Hubbard model. *Phys. Rev. B* **2016**, *94*, 195126. [CrossRef]
68. Feng, S. Kinetic energy driven superconductivity in doped cuprates. *Phys. Rev. B* **2003**, *68*, 184501. [CrossRef]
69. Wrobel, P.; Eder, R.; Micnas, R. Kinetic energy driven superconductivity and the pseudogap phase in weakly doped antiferromagnets. *J. Phys. Condens. Matter* **2003**, *15*, 2755. [CrossRef]
70. Guo, H.; Feng, S. Electronic structure of kinetic energy driven superconductors. *Phys. Lett. A* **2007**, *361*, 382. [CrossRef]
71. Otsuka, H. Variational Monte Carlo studies of the Hubbard model in one- and two-dimensions. *J. Phys. Soc. Jpn.* **1992**, *61*, 1645. [CrossRef]
72. Yanagisawa, T.; Koike, S.; Yamaji, K. *d*-wave state with multiplicative correlation factors for the Hubbard model. *J. Phys. Soc. Jpn.* **1999**, *68*, 3608. [CrossRef]
73. Eichenberger, D.; Baeriswyl, D. Superconductivity and antiferromagnetism in the-dimensional Hubbard model: A variational study. *Phys. Rev.* **2007**, *B76*, 180504. [CrossRef]
74. Baeriswyl, D.; Eichenberger, D.; Menteshashvii, M. Variational ground states of the two-dimensional Hubbard model. *New J. Phys.* **2009**, *11*, 075010. [CrossRef]
75. Baeriswyl, D. Superconductivity in the repulsive Hubbards model. *J. Supercond. Novel Magn.* **2011**, *24*, 1157. [CrossRef]
76. Capello, M.; Becca, F.; Fabrizio, M.; Sorella, S.; Tosatti, E. Variational description of Mott insulators. *Phys. Rev. Lett.* **2005**, *94*, 026406. [CrossRef] [PubMed]
77. Misawa, T.; Imada, M. Origin of high-T_c superconductivity in doped Hubbard models and their extensions: Roles of uniform charge fluctuations. *Phys. Rev.* **2014**, *B90*, 115137. [CrossRef]
78. Yanagisawa, T. Quantum Monte Carlo diagonalization for many-fermion systems. *Phys. Rev.* **2007**, *B75*, 224503. [CrossRef]
79. Deutscher, G.; Santander-Syro, A.F.; Bontemps, N. Kinetic energy change with doping upon superfluid condensation in high-temperature superconductors. *Phys. Rev.* **2005**, *B72*, 092504. [CrossRef]